PHYSICAL REVIEW E **79**, 041923 (2009)

Global noise and oscillations in clustered excitable media

X. L. Liao,[1] P. Jung,[2] and J. W. Shuai[3,*]
[1]*Department of Chemistry, College of Chemistry and Chemical Engineering, Xiamen University, Xiamen 361005, China*
[2]*Department of Physics and Astronomy and Quantitative Biology Institute, Ohio University, Athens, Ohio 45701, USA*
[3]*Department of Physics and Institute of Theoretical Physics and Astrophysics, Xiamen University, Xiamen 361005, China*
(Received 11 September 2008; published 24 April 2009)

We study the effects of global noise on waves in heterogeneous, spatially clustered, reaction-diffusion systems with possible applications to calcium signaling. We first discuss how clustering of the excitability determines the dynamics by shifting bifurcation points and creating new oscillatory solutions. We then consider the specific situation, where intrinsic noise, due to the smallness of the excitable patches, destroys the global oscillatory state. We show that additional small global fluctuations, however, can partially restore temporal and spatial coherence of the oscillatory signal.

DOI: 10.1103/PhysRevE.79.041923 PACS number(s): 87.16.Xa, 05.45.−a, 05.40.Ca

I. INTRODUCTION

Recently, considerable attention has been paid to the constructive effects of noise in nonlinear systems [1]. One of the widely studied phenomena is stochastic resonance and coherence resonance, where additional noise can improve a system's response to a weak periodic signal [2], or even in the absence of a periodic driving [3,4]. In complex biological systems, different sources of fluctuations are present, often characterized as extrinsic and intrinsic noises. It has been shown that intrinsic fluctuations can improve the encoding of small signals [5], or enhance the periodicity of spiking in a chain of coupled neurons [6]. Furthermore, multiple noise sources can generate novel and unexpected phenomena, such as effective noise cancellation [7], noise suppression by noise [8], or modulation of coherence resonance [9].

In this paper we discuss the synergistic effects of spatially independent and global fluctuations on a spatially clustered oscillating system. We show that a small optimal intensity of extrinsic, global noise can restore temporally and spatially coherent oscillations destroyed by intrinsic noise due to the smallness of the excitable clusters. In contrast to the standard stochastic-resonance scenario, where a deterministically stable (nonperiodic) state is turned into a periodic state, the coherence of a deterministically periodic state is enhanced by the interaction of various noises.

As a working model, we consider a model for intracellular calcium dynamics. This model used here does not contain biophysical details of the calcium signaling machinery, but is rather focused on the important consequences of clustering of excitability, an important source of intrinsic noise. Calcium ions are an important second messenger in living cells [10], and calcium signals have been subject of experimental [10–17] and theoretical investigations [18–29] in recent decades. Intracellular calcium is released from internal Ca^{2+} stores, most notably the endoplasmic reticulum (ER), through inositol 1,4,5-trisphosphate receptor channels (IP_3Rs). Recent experiments revealed that the IP_3Rs are distributed in clusters, spaced a few micrometers apart and with a few tens of channels per cluster [14]. Hence, Ca^{2+} liberation occurs at discrete release sites as puffs or sparks [11,13]. Each local release event is stochastic due to intrinsic stochasticity of channel opening and closing [11,13,14]. Local release events can merge to form global release events in the form of oscillations and waves.

It has been shown that rich and complex behaviors can be found in calcium dynamics, such as the shifts of bifurcations [30,31] and multiple stable states with hysteresis [32]. By investigating the global spike trains of four cell types, it has been suggested that Ca^{2+} spikes are caused by random wave nucleation with a regular regime arising from the array enhanced coherence resonance with IP_3R clusters [17]. Hence, the stochastic effects in such a system are not only curious from a physics perspective but are also relevant for open problems in cell biology. In Sec. IV of this paper, we show that the clustered organization of the release channels induces rich and complex dynamics of Ca^{2+} waves with a corresponding bifurcation diagram. We report in Secs. V and VI on a mechanism for generating spatially and temporally oscillations through the interaction of stochastic channel dynamics and global fluctuations of the concentration of the second messenger IP_3.

II. A SIMPLE MODEL FOR INTRACELLULAR CALCIUM DYNAMICS

We model the cytosolic space as a two-dimensional sheet, in which the calcium concentration, i.e., $C(x,y,t)$, is described by the following reaction-diffusion equation:

$$\frac{\partial C}{\partial t} = D\nabla^2 C + f(x,y)J_C - J_P + J_L, \tag{1}$$

where D denotes an effective diffusion constant, J_C channel flux from ER to the cytosol through clusters of IP_3Rs, J_P pump flux from the cytosol to ER through SERCA pumps, and J_L leakage flux from ER to the cytosol. The proteins that constitute pumps and leakage are assumed homogeneously distributed over the ER membrane. The IP_3Rs are distributed in clusters positioned on a regular lattice, described by the

*Corresponding author: FAX: +86 592-218-9426; jianweishuai@xmu.edu.cn

form-function $f(x,y)$ which is unity at the location of the clusters and zero elsewhere.

The three fluxes in Eq. (1) are given by

$$J_C = v_C g \frac{N_{\text{open}}}{N}(C_{\text{ER}} - C) \tag{2}$$

$$J_P = v_P \frac{C^2}{k^2 + C^2} \tag{3}$$

$$J_L = v_L(C_{\text{ER}} - C), \tag{4}$$

where C_{ER} describes the high concentration of Ca^{2+} in ER. For this study, which does not focus on physiologic detail, we assume that the concentration of Ca^{2+} in ER remains unchanged everywhere and is thus chosen to be a constant. The parameters v_C, v_P, and v_L describe the maximum flux through a cluster of IP_3Rs, maximum pump flux, and leakage rate, respectively. The flux J_C through a cluster (i) with N channels is determined by the fraction of open IP_3Rs in this cluster, i.e., $N^{(i)}_{\text{open}}/N$. For the gating of IP_3R, we use the Li-Rinzel model [19]. The Li-Rinzel model is a simplification of the DeYoung-Keizer model [18], in which each channel has three subunits with each a binding site for IP_3 (i.e., m-gate), and two binding sites for Ca^{2+}, one for activation (i.e., n-gate) and one for inactivation (i.e., h-gate). The channel is open if all three subunits are activated, i.e., IP_3 and activating Ca^{2+} are both bound. In the Li-Rinzel simplification, binding probabilities of IP_3 and activating Ca^{2+} are instantaneous and represented by their quasisteady states,

$$m_\infty = \frac{p}{p + d_m},$$

$$n_\infty = \frac{C}{C + d_n}, \tag{5}$$

where p represents the IP_3 concentration, giving rise to the factor $g = m_\infty^3 n_\infty^3$ in Eq. (2).

Ca^{2+}-inactivation (h-gate) is slow and described by the binding and dissociation rates α and β, given by

$$\alpha = a d_2 \frac{p + d_1}{p + d_3},$$

$$\beta = aC. \tag{6}$$

In case that the number of channels per cluster is large and the fluctuations are small, N_{open}/N can be replaced by the continuous fraction h, obeying the linear rate equations [19],

$$\frac{dh}{dt} = \alpha(1 - h) - \beta h. \tag{7}$$

The parameters k, d_m, d_n, d_1, d_2, d_3, and a in Eqs. (2)–(7) are specified in Table I.

Due to its large diffusion coefficient, IP_3 spreads out quickly through the cell after generated locally, acting as a global signal in the intracellular space [12] and is thus often treated as a common variable [20,21,24]. The dynamics of the IP_3 concentration p around its steady-state concentration p_0 are determined by [18],

$$\frac{dp}{dt} = \frac{p_0 - p}{\tau}, \tag{8}$$

with the degradation rate of $1/\tau$. According to [33], we chose $\tau = 10.0$ s here.

In this paper we will go one step further by taking into account stochasticity in the local production of IP_3 (e.g., through variable amounts of agonist binding to receptors on the plasma membrane), which through the rapid spread through the entire cell becomes a global, stochastic signal.

In our model, the IP_3Rs are distributed in equally sized clusters with $N = 36$ channels each, positioned on a regular array at a distance of $L = 3$ μm. The small size of the clusters facilitates rapid equilibration of calcium within the cluster and one can therefore assume that all channels in one cluster experience the same calcium concentration [20]. We further approximate the clusters as point sources where the actual size of the cluster appears as a prefactor of v_C [25], i.e., the form function $f(x,y)$ becomes a sum of δ functions located at the clusters. In the simulation, an area of 60×60 μm^2 membrane ER is discretized and represented by a grid with distance $\delta x = 0.5$ μm. Nonflux boundary conditions are applied in the model. The parameter values given in Ref. [24] are used in the present study (Table I).

TABLE I. Model parameters.

L	3 μm
N	36
D	15 $\mu m^2/s$
v_C	21.6 /s
v_P	0.5/s
v_L	0.001 μM/s
C_{ER}	15 μM
k	0.1 μM
d_m	0.13 μM
d_n	0.08 μM
a	0.2/μM/s
d_1	0.13 μM
d_2	1.05 μM
d_3	0.94 μM
τ	10 s

III. UNIFORM CALCIUM CONCENTRATION

In this section we discuss the behavior of the model in the limit of a large diffusion coefficient of Ca^{2+}, resulting in a rapid formation of a uniform Ca^{2+} concentration. All IP_3Rs of all clusters are clamped to the same, but variable, Ca^{2+} concentration. Thus, the Laplacian in Eq. (1) vanishes, the number N becomes the total number of channels 10 000, and the fraction N_{open}/N becomes continuous (h), leaving us with a set of ordinary differential equations for cytosolic Ca^{2+} concentration, i.e.,

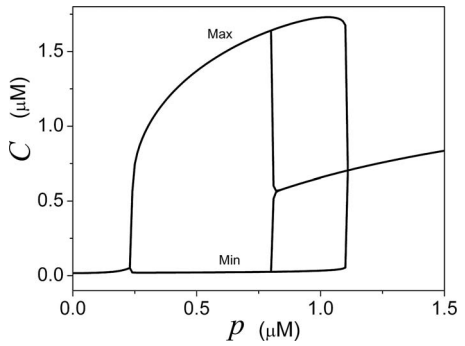

FIG. 1. Bifurcation diagram of the model as a function of IP_3 messenger p for intracellular calcium dynamics [Eqs. (1)–(7)] with uniform cytosolic Ca^{2+} concentration, i.e., for $D=\infty$. Oscillatory branches are depicted by the minimum and the maximum of the amplitude.

$$\frac{dC}{dt} = J_C - J_P + J_L,$$

$$\frac{dh}{dt} = \alpha(1-h) - \beta h, \tag{9}$$

where the channel flux becomes $J_C=\rho_C m_\infty^3 n_\infty^3 h^3 (C_{\mathrm{ER}}-C)$ with the modified maximum flux $\rho_C=\nu_C/36$ [24]. The other terms are the same as given in Eqs. (3)–(7). Stochastic effects of gating can be ignored here for the large number N (fluctuations are of the $1/\sqrt{N_{\mathrm{Total}}}$) [22].

For this deterministic model [Eq. (9)], the bifurcation diagram of stable attractors of Ca^{2+} signal is shown in Fig. 1 as a function of p. For IP_3 concentrations p, between 0.24 μM and 1.1 μM, Ca^{2+} oscillations are observed, while for lower and higher IP_3 concentrations, stationary concentrations are found. This bifurcation diagram sets the stage for further studies of the behavior of the system without the constraints to large diffusion coefficients of Ca^{2+} and large numbers of channels.

IV. CHANNEL-CLUSTERING AND DYNAMIC BIFURCATIONS IN THE ABSENCE OF STOCHASTIC EFFECTS

We now lift the constraint of a large diffusion coefficient and allow for gradients in the overall Ca^{2+} concentration. We do, however, at this point neglect stochasticity in the cluster conductance due to spontaneous opening and closing of IP_3Rs. Hence, we consider the deterministic dynamics and pattern formation in a spatially clustered excitable system.

To quantify the effects of spatial gradients for the dynamics and stable attractors, we consider the dynamics of cell-averaged Ca^{2+} concentrations, i.e., we solve Eqs. (1)–(5) and then perform a spatial average. In Figs. 2(A) and 2(B) we show the bifurcation diagrams of cell-averaged calcium C_{Cell} as a function of p at $D=30$ and 15 $\mu m^2/s$, respectively. These diffusion coefficients are biologically meaningful as they incorporate the effect of buffers [12].

At $D=30$ $\mu m^2/s$ the dynamic behavior resembles very much the system with uniform Ca^{2+} concentrations, i.e., the

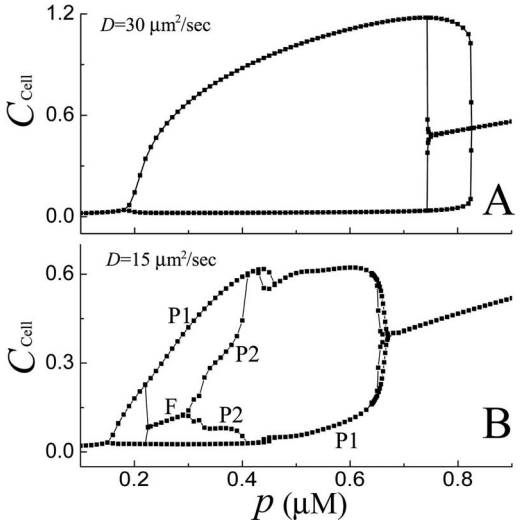

FIG. 2. Bifurcation diagrams of the model for intracellular calcium dynamics [Eqs. (1)–(7)] for nonuniform cytosolic Ca^{2+} concentration and clustered arrangement of the IP_3Rs with a cluster distance of 3 μm for $D=30$ $\mu m^2/s$ (a), and $D=15$ $\mu m^2/s$ (b). Channel dynamics are deterministic. Stable oscillatory branches are depicted by the minimum and the maximum of the amplitude. P1 and P2 denote oscillatory branches while F denotes the fix point.

oscillations of Ca^{2+} signal are found for the range of $0.18\ \mu M < p < 0.84\ \mu M$. The minimum and the maximum amplitudes in Fig. 2 depict oscillations. The onset and termination of oscillations are shifted to smaller values of p.

At $D=15$ $\mu m^2/s$, however, we find a bifurcation diagram which is qualitatively very different [Fig. 2(B)]. The range of IP_3 concentrations for which we find stable oscillations is even smaller, and the bistable range (a fixed point and an oscillatory attractor) just before the bifurcation back to steady state (i.e., close to $p>0.69$ μM) has shrunk [Fig. 2(B)]. Most interestingly, however, a new steady-state branch F in the interval $0.15\ \mu M < p < 0.23\ \mu M$ and a new oscillatory branch P_2 in the interval $0.23\ \mu M < p < 0.29\ \mu M$ emerged. The new branch of fixed point F coexists with the oscillatory state P_1. Closer inspection of the spatiotemporal patterns represented by P_1 and P_2 shows that these are two phase shifted, propagating intracellular Ca^{2+} waves (data not shown).

In the following, we focus our attention to the region of $0.23\ \mu M < p < 0.29\ \mu M$, where a propagating Ca^{2+} wave (P1) coexists with a steady-state concentration. We will next take into account intrinsic channel noise and global fluctuations in the IP_3 concentration p, and study the fate of the spatiotemporal dynamics of calcium signal. We will show that the channel noise alone will destroy the wave and the associated spatial and temporal coherence. Small global fluctuations of IP_3, however can partially restore temporal and spatial coherence of the intracellular calcium oscillation.

V. Ca^{2+} SIGNALING MODEL WITH INTRINSIC CHANNEL NOISE

For a small number of channels in each cluster, the fraction of open channels in a cluster is stochastic due to the

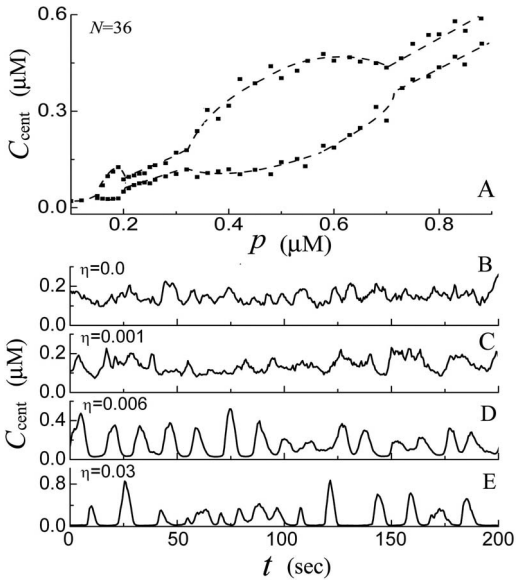

FIG. 3. (a) Bifurcation diagrams of the model for intracellular calcium dynamics [Eqs. (1)–(7)] for nonuniform cytosolic Ca^{2+} concentration and clustered arrangement of the IP_3Rs with 36 channels per cluster and a cluster distance of 3 μm at $D=15$ $\mu m^2/s$. In contrast to Fig. 2, stochastic channel open/closing dynamics have been taken into account. Oscillatory branches are depicted by the minimum and the maximum of the amplitude. In [(B)–(E)] we show traces of Ca^{2+} concentrations at the center cluster for increasing noise intensities of the second messenger IP_3 at $\eta=0.0$, 0.001, 0.006 and 0.03, respectively. Here $p_0=0.25$ μM.

thermal opening and closing [22] of the individual channels. In this case, the channel fluxes at the various cluster sites (i) can be expressed as

$$J_C^{(i)} = v_{Cg}\frac{N_{h\text{-Open}}^{(i)}}{N}(C_{ER} - C^{(i)}), \tag{10}$$

where $N_{h\text{-Open}}^{(i)}$ denotes the number of noninhibited IP_3Rs of cluster (i), and $C^{(i)}$ the cytosolic calcium concentration at cluster site (i). In order to determine the number $N_{h\text{-Open}}^{(i)}$, we perform a Markov-simulation of the gating scheme of IP_3Rs as described in [22] with the binding and dissociation rates given in Eq. (6).

We combine the Markov simulations of the clusters with 36 IP_3Rs per cluster with the solution of Eq. (1) to find the stochastic spatiotemporal Ca^{2+} dynamics. Averaging the noisy Ca^{2+} concentrations over the entire system we can compare the resulting bifurcation diagram [Fig. 3(A)] with that obtained in the absence of channel noise at $D=15$ $\mu m^2/s$ [Fig. 2(B)]. Some of the detail of the nonstochastic bifurcation diagram [Fig. 2(B)] vanishes in the presence of channel noise. The two branches P_1 and P_2 in Fig. 2(B) describing propagating calcium waves merge into a single state. The steady-state branch F in Fig. 2(A) merges with P_1 to yield stochastic calcium fluctuation around the steady state [see Fig. 3(B)]. The power spectrum of calcium fluctuation at $p_0=0.25$ μM indicates little periodicity, as shown in Fig. 4 ($\eta=0$). The coherence and periodicity of the intracellular Ca^{2+} wave signal are destroyed by the spatially

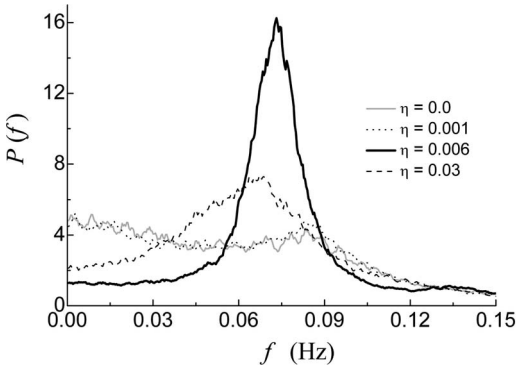

FIG. 4. The normalized power spectra of Ca^{2+} concentrations $C_{cent}(t)$ at central cluster in the two-dimensional (2D) cell model are calculated with different IP_3 noise intensities, i.e., $\eta=0$ (thin solid line), 0.001 (dotted line), 0.006 (thick solid line), and 0.03 $\mu M/s^{1/2}$ (dashed line). Here $p_0=0.25$ μM and $N=36$.

independent fluctuations of channel conductance. In Sec. VI, we show that an optimal amount of extrinsic fluctuations in the global IP_3 concentration can restore the temporally and spatially coherent Ca^{2+} waves, which were destroyed by the channel noise at $p_0=0.25$ μM.

VI. INTERACTION BETWEEN INTRINSIC CHANNEL NOISE AND EXTRINSIC IP_3 FLUCTUATION

We now take into account global stochasticity of the IP_3 concentration p. Global IP_3 fluctuations are likely to occur whenever IP_3 is generated as a response to extracellular agonist binding to metabotropic receptors distributed locally on the plasma membrane or through local release of caged IP_3 through application of light in experiment [11,14].

Assuming a narrow Gaussian distribution of the IP_3 concentration around the average value of $p_0=0.25$ μM, the dynamics of p is described by the stochastic differential equation,

$$\frac{dp}{dt} = \frac{p_0 - p}{\tau} + \eta\xi(t), \tag{11}$$

where η denotes the noise strength, and $\xi(t)$ white Gaussian noise with zero mean, i.e.,

$$\langle \xi(t) \rangle = 0$$

$$\langle \xi(t_1)\xi(t_2) \rangle = 2\delta(t_1 - t_2). \tag{12}$$

Artifacts such as negative values for p do not typically occur since we only use small values of η. The variance of the Gaussian distribution of p is given by $\tau\eta^2$. Hence for $\eta=0.03$, i.e., the largest value of η we are using, one has $\tau\eta^2=0.009$ μM^2. Thus, the standard deviation $\sqrt{\tau\eta^2}=0.095$ μM, which is much smaller than the average $p_0=0.25$ μM, and so the chance of negative values of p is very small.

In Figs. 3(C)–3(E), we show the effect of global fluctuations of IP_3 on the calcium dynamics at the center cluster of the cell model for various fluctuation strengths η. Visible

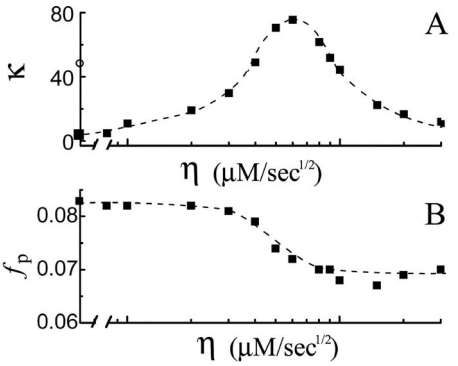

FIG. 5. The periodicity factor κ [Eq. (13)] of the Ca^{2+} signal $C_{cent}(t)$ at central cluster (a) and the corresponding peak frequency of the power spectrum (b) are plotted as a function of IP_3 noise intensity η.

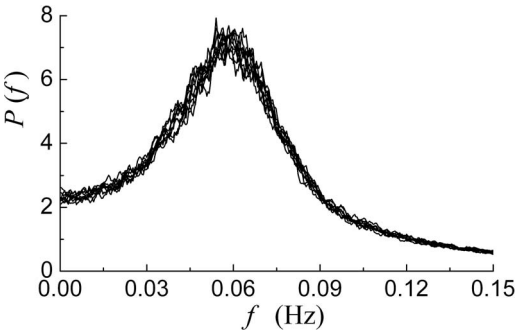

FIG. 6. The normalized power spectra of Ca^{2+} concentrations $C_{cent}(t)$ for an independent cluster (i.e., a stochastic point model only) are calculated with different IP_3 noise intensities at η=0.0, 0.001, 0.002, 0.004, 0.006, 0.008, 0.01, 0.02, and 0.03. Here p_0 =0.25 μM and N=36.

inspection of the data suggests that an increase in global IP_3 fluctuation results in a more periodic Ca^{2+} signal with an optimal value of about η=0.006 $\mu M/s^{1/2}$ [Fig. 3(D)]. Hence periodicity and signal encoding are restored at an optimal value of IP_3 fluctuation. Comparing the normalized power spectra of the calcium trajectories of the center cluster we further assess this effect. The corresponding power spectra are shown in Fig. 4 for trajectories at η=0.0, 0.001, 0.006, and 0.03 $\mu M/s^{1/2}$. The spectrum at η=0.006 $\mu M/s^{1/2}$ clearly demonstrates the restored periodicity at a frequency of 0.075 Hz.

The periodicity of the Ca^{2+} signal can be characterized by

$$\kappa = H_P \frac{f_p}{\Delta f}, \tag{13}$$

where H_p represents the peak height of the spectrum $P(f)$, f_p the frequency at the peak, and Δf the frequency width at half peak height. A larger value of κ indicates a better periodicity [3]. Figure 5(A) shows that the periodicity first increases with increasing global fluctuations η, reaching a maximum at η=0.006 $\mu M/s^{1/2}$, and then decreases with larger η.

The peak frequency is also shifted with increasing η as shown in Fig. 5(B). At small η the peak frequency is about 0.087 Hz, while at large η the peak frequency approaches to 0.07 Hz, which is close to the oscillation frequency of the system in the absence of any noise (i.e., 0.067 Hz).

VII. DISCUSSION AND CONCLUSIONS

We have found that global noise, generated through rapid diffusion of the second messenger IP_3, can restore global periodicity of the cellular Ca^{2+} signal, which has been destroyed by channel conductance fluctuations, and hence increase cellular signaling capability. In this section we discuss the underlying mechanism for this unexpected behavior.

To explain this effect, we consider first a single cluster of IP_3Rs in the absence of interaction with other clusters in the presence of channel noise and IP_3 fluctuation. This is realized by considering one cluster and setting the diffusion constant zero. More concrete, we solve Eq. (1) with D=0, the channel flux given in Eq. (10) with a cluster size of N=36 channels, and the stochastic differential equation for IP_3 concentration p given in Eq. (11). In Fig. 6, we show the power spectra of the single cluster for a range of fluctuation intensities η of the IP_3 concentration. All power spectra are very similar and do not show an increase in periodicity at any value of η. Hence, the dynamics of a single cluster is not the origin of the increase in global periodicity in the presence of coupling to other clusters.

To further substantiate the hypothesis that the increased periodicity is related to the diffusive coupling between clusters, we study the correlation between local Ca^{2+} dynamics at the center cluster C_{cent} and the global cell-averaged Ca^{2+} dynamics C_{cell}, i.e.,

$$F(\tau) = \frac{\langle (C_{cell}(t) - \langle C_{cell} \rangle) \cdot (C_{cent}(t) - \langle C_{cent} \rangle) \rangle}{\sqrt{\langle (C_{cell}(t) - \langle C_{cell} \rangle)^2 \rangle \cdot \langle (C_{cent}(t) - \langle C_{cent} \rangle)^2 \rangle}}. \tag{14}$$

A simple measure for the overall correlation is the correlation time [24],

$$\tau_0 = \int_0^\infty F^2 dt, \tag{15}$$

which is shown in Fig. 7 for the model discussed in Figs. 4 and 5. The correlation time increases with increasing global IP_3 fluctuations until it reaches a maximum at the same value where the local Ca^{2+} dynamics are most periodic (see Fig. 4).

Hence, periodicity is linked to large spatial correlations, allowing a simple interpretation of the main result in this paper. Global IP_3 fluctuations, although small, slightly bias

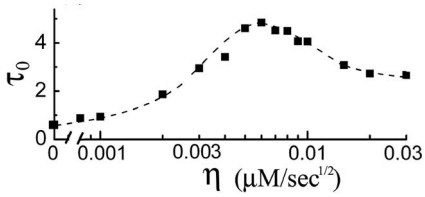

FIG. 7. The cross-correlation time τ_0 [Eq. (15)] between $C_{cent}(t)$ and $C_{Cell}(t)$ are plotted as a function of IP_3 noise intensity η for the model given in Figs. 4 and 5.

the clusters to correlated occurrence of Ca^{2+} release. Ca^{2+} released at one site diffuses to other nearby clusters and further correlates the clusters through calcium-induced calcium release.

In the paper we report an unexpected effect of global fluctuations in a clustered excitable medium. We show that spatiotemporal coherence, destroyed by the fluctuations borne by the small size of the number of ion channels in a cluster generating the excitability, can be partly restored by global fluctuations acting on all excitable clusters of the system.

This effect has been studied in a simple model for calcium signaling which does not contain much biophysical detail. For example, we ignore suspected large gradients in the calcium concentrations in the vicinities of open channels and their consequences for the onset of oscillations. It thus remains an open problem how robust this effect is and whether it maybe relevant for intracellular calcium signaling.

ACKNOWLEDGMENTS

P.J. thanks for funding by the U.S. National Science Foundation through Grant No. IOS-0744798. J.W.S. thanks for funding by the National Science Foundation of China through Grant No. 10775114.

[1] C. V. Rao, D. M. Wolf, and A. P. Arkin, Nature (London) **420**, 231 (2002).
[2] L. Gammaitoni, P. Hanggi, P. Jung, and F. Marchesoni, Rev. Mod. Phys. **70**, 223 (1998).
[3] Hu Gang, T. Ditzinger, C. Z. Ning, and H. Haken, Phys. Rev. Lett. **71**, 807 (1993).
[4] A. S. Pikovsky and J. Kurths, Phys. Rev. Lett. **78**, 775 (1997).
[5] P. Jung and J. W. Shuai, Europhys. Lett. **56**, 29 (2001).
[6] C. S. Zhou, J. Kurths, and B. Hu, Phys. Rev. Lett. **87**, 098101 (2001).
[7] K. P. Singh, G. Ropars, M. Brunel, and A. Le Floch, Phys. Rev. Lett. **90**, 073901 (2003).
[8] J. M. G. Vilar and J. M. Rubi, Phys. Rev. Lett. **86**, 950 (2001).
[9] G. Yu, M. Yi, Y. Jia, and J. Tang, Chaos, Solitons Fractals (unpublished).
[10] M. J. Berridge, M. D. Bootman, and P. Lipp, Nature (London) **395**, 645 (1998).
[11] I. Parker and Y. Yao, Proc. R. Soc. London, Ser. B **246**, 269 (1991).
[12] N. L. Allbritton, T. Meyer, and L. Stryer, Science **258**, 1812 (1992).
[13] H. Cheng, W. J. Lederer, and M. B. Cannell, Science **262**, 740 (1993).
[14] X. P. Sun, N. Callamaras, J. S. Marchant, and I. Parker, J. Physiol. (Paris) **509**, 67 (1998).
[15] R. Miledi, I. Parker, and G. Schalow, Nature (London) **268**, 750 (1977).
[16] J. K. Foskett, C. White, K. H. Cheung, and D. O. Mak, Physiol. Rev. **87**, 593 (2007).
[17] A. Skupin, H. Kettenmann, U. Winkler, M. Wartenberg, H. Sauer, S. C. Tovey, C. W. Taylor, and M. Falcke, Biophys. J. **94**, 2404 (2008).
[18] G. W. De Young and J. Keizer, Proc. Natl. Acad. Sci. U.S.A. **89**, 9895 (1992).
[19] Y. Li and J. Rinzel, J. Theor. Biol. **166**, 461 (1994).
[20] S. Swillens, G. Dupont, L. Combettes, and P. Champeil, Proc. Natl. Acad. Sci. U.S.A. **96**, 13750 (1999).
[21] M. Falcke, L. S. Tsimring, and H. Levine, Phys. Rev. E **62**, 2636 (2000).
[22] J. W. Shuai and P. Jung, Biophys. J. **83**, 87 (2002).
[23] B. Pando, J. E. Pearson, and S. P. Dawson, Phys. Rev. Lett. **91**, 258101 (2003).
[24] J. W. Shuai and P. Jung, Proc. Natl. Acad. Sci. U.S.A. **100**, 506 (2003).
[25] J. W. Shuai and P. Jung, Phys. Rev. E **67**, 031905 (2003).
[26] N. Guisoni and M. J. de Oliveira, Phys. Rev. E **74**, 061905 (2006).
[27] Y. B. Yi, H. Wang, A. M. Sastry, and C. M. Lastoskie, Phys. Rev. E **72**, 021913 (2005).
[28] J. Shuai, H. J. Rose, and I. Parker, Biophys. J. **91**, 4033 (2006).
[29] M. A. Huertas and G. D. Smith, J. Theor. Biol. **246**, 332 (2007).
[30] R. Thul and M. Falcke, Phys. Biol. **2**, 51 (2005).
[31] R. Thul and M. Falcke, Phys. Rev. Lett. **93**, 188103 (2004).
[32] J. M. A. M. Kusters, J. M. Cortes, W. P. M. van Meerwijk, D. L. Ypey, A. P. R. Theuvenet, and C. C. A. M. Gielen, Phys. Rev. Lett. **98**, 098107 (2007).
[33] S. S.-H. Wang, A. A. Alousi, and S. H. Thompson, J. Gen. Physiol. **105**, 149 (1995).